Biochem. J. (1989) 262, 773–779 (Printed in Great Britain)

The intrinsic tryptophan fluorescence of β_1-bungarotoxin and the Ca^{2+}-binding domains of the toxin as probed with Tb^{3+} luminescence

Sin-Tak CHU and Yee-Hsiung CHEN*

Institute of Biochemical Science, College of Science, National Taiwan University, and Institute of Biological Chemistry, Academia Sinica, Taipei, 10764 Taiwan, Republic of China

β_1-Bungarotoxin has only one tryptophan residue, namely Trp-19 in the phospholipase A_2 subunit. The environment of Trp-19 was studied by intrinsic fluorescence and solute quenching. The native protein showed an emission peak at 330 nm. About 90% of the fluorescent tryptophan was accessible to quenching by either acrylamide or KI but not to CsCl. A red-shift in the emission peak occurred between 2.0 M- and 4.0 M-guanidinium chloride, and the helix–coil transition of the polypeptide backbone occurred between 4.0 M- and 6.0 M-guanidinium chloride. These results suggested that Trp-19 was in a less polar medium but near a positive charge. The local conformation around Trp-19 could be disturbed by binding of Tb^{3+} or Ca^{2+} or Sr^{2+} to the toxin molecule. Tb^{3+} a tervalent lanthanide ion, effectively substituted for Ca^{2+} in stimulating the phospholipase A_2 activity of β_1-bungarotoxin. Upon the binding of Tb^{3+} to the toxin, the Tb^{3+} fluorescence in the 450–650 nm region was enhanced. This resulted from the energy transfer from Trp-19 to Tb^{3+}. The distance between the energy-transfer pair was estimated to be 0.376–0.473 nm at pH 7.6 and 0.486–0.609 nm at pH 6.3. Assuming that there were two Tb^{3+}-binding sites on the toxin molecule, at pH 7.6 the association constants of the high-affinity and the low-affinity sites were determined to be 3.82×10^3 M^{-1} and 2.85×10^2 M^{-1} respectively. At between pH 6.0 and 7.0 Tb^{3+} bound to the high-affinity site decreased greatly but did not disappear entirely. Both Ca^{2+} and Sr^{2+} competed with Tb^{3+} at the high-affinity sites, but Sr^{2+} could not substitute for Ca^{2+} in stimulating the phospholipase A_2 activity.

INTRODUCTION

The presynaptically active toxins in the venom of snakes belonging to Elapidae, Crotalidae and Viperidae are very potent in blocking neuromuscular transmission (Chang, 1985). Since their action is very specific and unique, they have been exploited as important tools or probes in physiological, biochemical and pharmacological studies. β_1-Bungarotoxin (β_1-BuTx), the main component of β-bungarotoxins in the venom of the Taiwan banded krait (*Bungarus multicinctus*) (Chen *et al.*, 1982), is a representative of this kind of toxin. It induces firstly facilitation and then irreversible disruption of acetylcholine release from the cholinergic synapses before the blockade of neuromuscular transmission. The toxin consists of two polypeptide chains linked by a disulphide bond (Kondo *et al.*, 1978*b*). One polypeptide chain is a phospholipase A_2 (PLA_2) subunit having 120 amino acid residues (Fig. 1), which shows sequence similarity to other vertebrate PLA_2 enzymes (Kini & Evans, 1987). This subunit is believed to play the key role in causing the neurotoxicity. The other is a rather small subunit with 60 amino acid residues. Its role in the neurotoxic effect is currently unclear, despite the fact that it shows sequence similarity to dendrotoxin and toxins I and K from the venom of mamba, which are representatives of Kunitz proteinase inhibitors (Dufton, 1985) and themselves show facilitation of transmitter release, interference with the binding of native β-BuTX in chick muscle and enhancement of the presynaptic effect of crotoxin and notexin (Harvey & Karlsson, 1982).

Establishing the nature of the Ca^{2+}-binding domains in the β_1-BuTx molecule is important in elucidating the structure–function relationship of the protein molecule. Thus far, the association constant of the toxin–Ca^{2+} complex has been estimated from a binding assay using radioactive Ca^{2+} or from the effect of the metal ion on the optical properties of toxin (Abe *et al.*, 1977; Ikeda & Hayashi, 1983). However, these approaches are limited to exploring the configuration around the Ca^{2+}-binding domain. For one thing, Ca^{2+} is devoid of useful spectroscopic characteristics that can be employed in probing the nature of its binding site. For another, analysis of the Ca^{2+}-induced change of the optical properties provides little information when the chromophore(s) responsible for the spectral change is not included in or not proximal to the ion-binding domain.

Tervalent lanthanide ions have in common with Ca^{2+} an ionic radius of about 0.1 nm and co-ordination number between 6 and 8 (Prados *et al.*, 1974). In recent years Tb^{3+} has been demonstrated to be an excellent probe for studying the binding domain of Ca^{2+} in a protein molecule (Epstein *et al.*, 1974; Gergely *et al.*, 1981). The present work investigates the intrinsic fluorescence due to the tryptophan residue of β_1-BuTx and the characteristics of the β_1-BuTx–Tb^{3+} complex.

Abbreviations used: β_1-BuTx, β_1-bungarotoxin; PLA_2, phospholipase A_2.

* To whom correspondence should be addressed.

EXPERIMENTAL

Materials

Crude venom of the Taiwan banded krait was supplied by Chen Hsin Tong Chemical Co., Taipei, Taiwan. CM-Sephadex C-25 and Sephadex G-50 were obtained from Pharmacia, Uppsala, Sweden. $TbCl_3$ was purchased from Alfa Products, Thiokol, MA, U.S.A. All other chemicals were of reagent grade. β_1-BuTx was isolated from the crude venom on a CM-Sephadex C-25 column (Chen *et al.*, 1982) and purified further on a Sephadex G-50 column (Lin *et al.*, 1984).

Assay of PLA_2 activity

PLA_2 activity was determined by two methods. In the first method the release of fatty acid from 10.0 μmol of egg phosphatidylcholine suspended in 4.0 ml of 5.0 mM-deoxycholate at 37 °C was measured by H^+ titration, which was carried out with a Radiometer pHM8 standard pH-meter attached to a T80 titrator and an ABU80 autoburette. One unit of PLA_2 activity was defined as the release of 1 μequiv. of fatty acid from phospholipid/min. In the second method the synergistic effect of PLA_2 on the haemolysis induced by snake-venom cardiotoxin was evaluated. The haemolysis assay followed the method used previously (Chen *et al.*, 1987).

C.d. and fluorescence

The concentration of β_1-BuTx was determined from the absorbance at 280 nm, by using $A^{1\%}_{1cm} = 12.5$ (Lin *et al.*, 1978*a*). The fluorescence intensity, expressed in spectropolarimeter under constant flushing with N_2 at room temperature. The mean residue ellipticity, $[\theta]$, was estimated from a mean residue weight of 166.7, which was calculated from the amino acid composition (Kondo *et al.*, 1978*a*). The fluorescence intensity, expressed in arbitrary units, was measured with a Hitachi MPF-4 fluorescence spectrophotometer.

Analyses of fluorescence data

The fluorescence data of β_1-BuTx in the presence of quenchers were analysed by the modified Stern–Volmer plot (Lehrer, 1971):

$$\frac{F_0}{F_0-F} = \frac{1}{F_a} + \frac{1}{F_a K_q[\phi]} \quad (1)$$

where F_0 and F are the fluorescence intensities of the protein in the absence and in the presence of quencher respectively, $[\phi]$ is the quencher concentration, K_q is the Stern–Volmer quenching constant and F_a is the fraction of fluorescent groups accessible to the quencher. A plot of $F_0/(F_0-F)$ versus $1/[\phi]$ will yield a straight line whose slope is $(F_a K_q)^{-1}$ and intercept is $1/F_a$.

The actual distance between donor and acceptor chromophores, R, of an energy-transfer pair was calculated from the equation:

$$R = R_0\left(\frac{1-E}{E}\right)^{-6} \quad (2)$$

where E is the efficiency of the energy-transfer process and R_0 is the distance when E is 50%. E was calculated by using the following relationship (Freifelder, 1982):

$$E = \left(\frac{\epsilon_1^A C^A}{\epsilon_1^D C^D}\right)\left(\frac{F_{1,2}^{D,A}}{F_{1,2}^A}\right) - 1 \quad (3)$$

where ϵ_1^A and ϵ_1^D are the molar absorption coefficients of acceptor and donor at λ_1 wavelength respectively, C^A and C^D are the concentrations of acceptor and donor respectively, and $F_{1,2}^A$ and $F_{1,2}^{A,D}$ are the fluorescence intensities of acceptor and the donor–acceptor pair respectively at λ_2 wavelength when excited at λ_1 wavelength. λ_1 is chosen so that absorption by the donor is efficient but that by the acceptor is inefficient. λ_2 is a wavelength at which there is emission only by the acceptor. R_0 was calculated according to Forster's (1959) theory:

$$R_0 = 9.79 \times 10^2 (J n^{-4} K^2 Q_0)^{-6} \text{ nm} \quad (4)$$

where J is the spectral-overlap integral, n is the refractive index of the medium between donor and acceptor, K is the orientation factor of the dipole pair, and Q_0 is the absolute quantum yield of the fluorescent donor in the absence of acceptor. The Q_0 value of β_1-BuTx was determined by comparison with the known quantum yield of quinine sulphate. J was calculated directly from spectral information according to the following equation:

$$J = \frac{\int F(\lambda)\epsilon(\lambda)\lambda^2 \cdot d\lambda}{\int F(\lambda)\lambda^{-2} \cdot d\lambda} \quad (5)$$

where F is the fluorescence intensity of donor and ϵ the molar absorption coefficient of acceptor.

The modified Scatchard plot (Epstein *et al.*, 1974) was constructed to analyse the fluorescence data of the β_1-BuTx–Tb^{3+} complex:

$$F/[Tb^{3+}]_{free} = (K_T \cdot F_\infty) - (K_T \cdot F) \quad (6)$$

where F is the fluorescence intensity of Tb^{3+} in the presence of β-BuTx, F_∞ is the fluorescence at infinite Tb^{3+} concentration, and K_T is the association constant of the β_1-BuTx–Tb^{3+} complex. Throughout the titration, $F/[Tb^{3+}]_{total}$ was plotted against F, since $[Tb^{3+}]_{free}$ was close to $[Tb^{3+}]_{total}$.

When a solution containing a suitable amount of β_1-BuTx and $TbCl_3$ was titrated with the same solution in the presence of metal ion L, the fluorescence data were analysed by a normalized Scatchard equation (Epstein *et al.*, 1974):

$$\bar{Y}_L/[L] = K_L - K_L(\bar{Y}_L + \bar{Y}_{Tb^{3+}}) \quad (7)$$

where $\bar{Y}_L$ and $\bar{Y}_{Tb^{3+}}$ are the fractions of saturation with respect to L and Tb^{3+}, and K_L is the association constant for formation of the complex between β_1-BuTx and metal ion L.

RESULTS

Status of tryptophan residue of β_1-BuTx

β_1-BuTx has only one tryptophan residue, namely Trp-19 of the PLA_2 subunit (Fig. 1). Fig. 2 displays the emission spectra of β_1-BuTx under several conditions. Excitation was at 295 nm to ensure that the fluorescence would be due to Trp-19. The native protein in 0.02 M-Pipes buffer at pH 7.6 (Fig. 2, curve I) exhibited a peak at 330 nm. The peak shifted to 342 nm and the intensity increased when the protein was in 6.0 M-guanidinium chloride (Fig. 2, curve II). Further cleavage of the disulphide bonds of the protein with dithiothreitol shifted the peak to 347 nm (Fig. 2, curve III). These spectral characteristics indicate that Trp-19 is restricted in

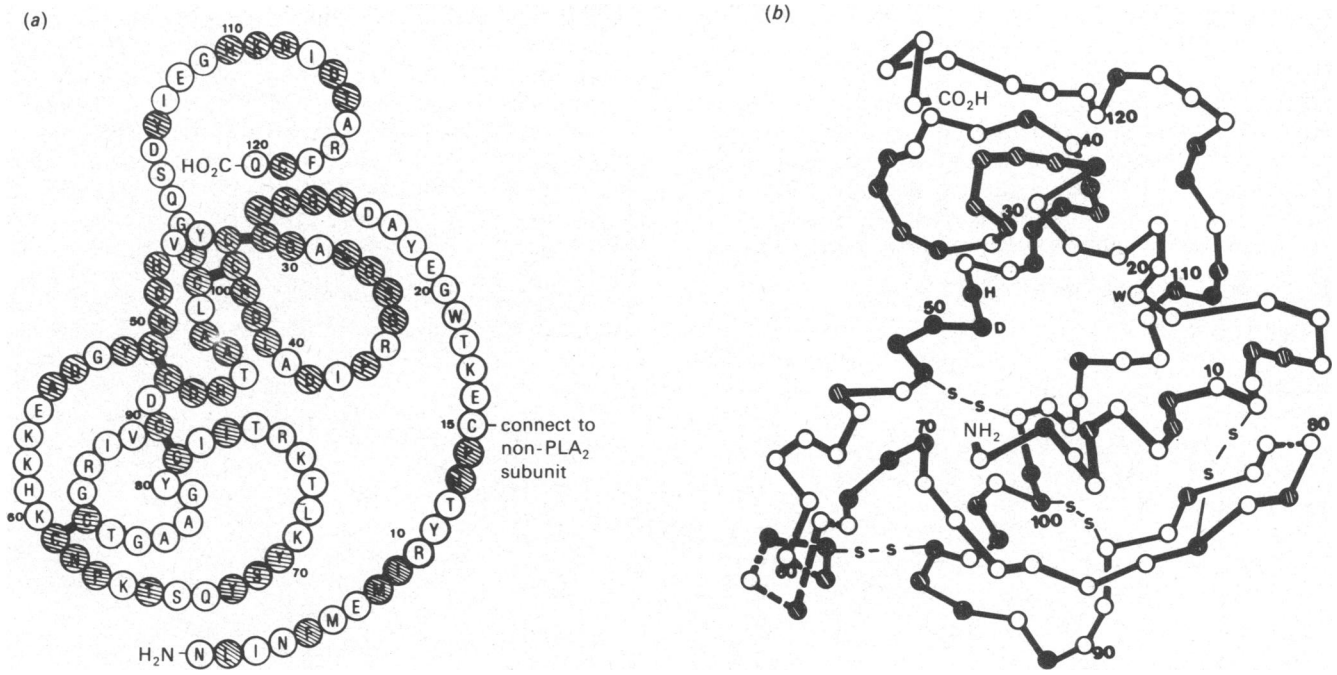

Fig. 1. (*a*) Primary structure of the PLA_2 subunit of β_1-BuTx [drawn essentially according to the schematic drawing described by Verheij *et al.* (1981) and Kondo *et al.* (1982)] and (*b*) superimposition of the primary structure of PLA_2 subunit of β_1-BuTx on to the main-chain conformation of bovine pancreatic PLA_2 (Dijkstra *et al.*, 1978)

Broken lines indicate the main points of variance between pancreatic and *Crotalus atrox* PLA_2 enzymes. In both (*a*) and (*b*) hatched circles indicate invariant residues in vertebrate PLA_2 enzymes according to the comparison made by Kini & Evans (1987).

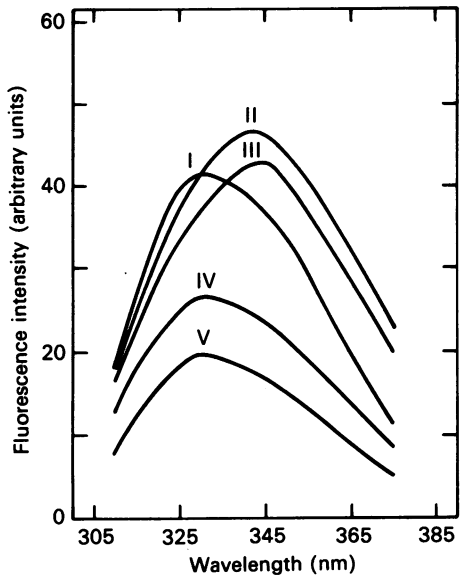

Fig. 2. Fluorescence emission spectra of β_1-BuTx in several solutions at pH 7.6

Curve I, spectrum in 0.02 M-Pipes; curve II, spectrum in 6.0 M-guanidinium chloride; curve III, spectrum in 6.0 M-guanidinium chloride in the presence of 0.1 mM-dithiothreitol; curve IV, spectrum in 0.1 M-KI; curve V, spectrum in 1.0 M-acrylamide. The toxin (5.0 μM) was excited at 295 nm.

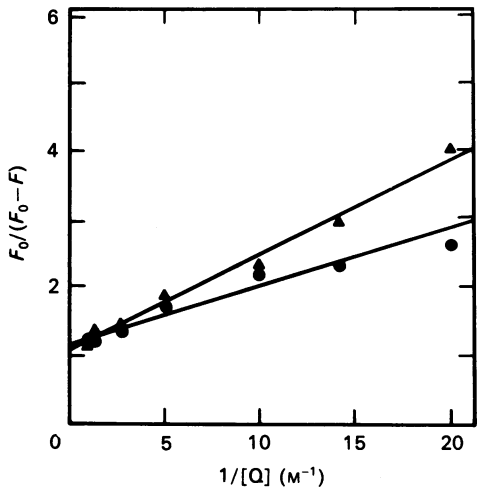

Fig. 3. Susceptibility of the tryptophan residue of β_1-BuTx towards KI and acrylamide

The fluorescence data for 5.0 μM-β_1-BuTx were treated in accordance with eqn. (1) described in the text. Symbols: ▲, in KI solution; ●, in acrylamide solution.

a configuration that differs from the status of free tryptophan in aqueous solution.

Both KI and acrylamide quenched the fluorescence, but they caused no shift of the emission peak (Fig. 2, curves IV and V). On the other hand, CsCl exerted no such quenching effect (results not shown). About $91.0 \pm 3.5\%$ and $89.0 \pm 2.3\%$ of Trp-19 was apparently accessible to KI and acrylamide respectively, on the basis of the plot according to eqn. (1) (Fig. 3).

Fig. 4 shows both fluorescence intensity and $[\theta]_{220}$ of β_1-BuTx in 0–6 M-guanidinium chloride. The emission

peak remained at 330 nm and the fluorescence intensity changed slightly at concentrations less than 2.0 M-guanidinium chloride. The peak shifted to 342 nm and the intensity increased remarkably in the concentration range 2.0–4.0 M-guanidinium chloride but levelled off in the concentration range 5.0–6.0 M-guanidinium chloride. In contrast, the helix–coil transition of the polypeptide backbone, as reflected by the change in $[\theta]_{220}$, occurred in the concentration range 4.0–6.0 M-guanidinium chloride.

Fluorescence of the β_1-BuTx–Tb^{3+} complex

Fig. 5 gives the fluorescence spectra of Tb^{3+} at pH 7.0 and 7.6. The emission spectrum showed a distinct quartet between 450 and 650 nm. Several peaks appeared at 265, 280, 320, 350 and 372 nm in the excitation spectrum in the region 250–400 nm. Each peak in either the excitation or the emission spectrum was pH-dependent. The higher the pH value, the higher the intensity (cf. curves ····· and –·–·– of Fig. 5). The intensity of Tb^{3+} fluorescence was markedly enhanced by the presence of β_1-BuTx. At higher pH values, more of the Tb^{3+} fluorescence was enhanced (cf. Fig. 5, curves ····· and ---- and curves –·–·– and ——).

The enhancement of Tb^{3+} fluorescence by β_1-BuTx was represented in terms of a ratio of Tb^{3+} fluorescence

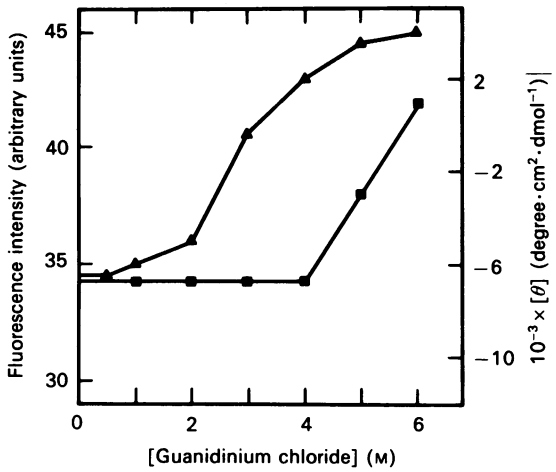

Fig. 4. Flexibility of tryptophan configuration and the polypeptide backbone folding of β_1-BuTx in guanidinium chloride solution

Fluorescence intensity was measured at 342 nm (▲). C.d. was measured at 220 nm (■).

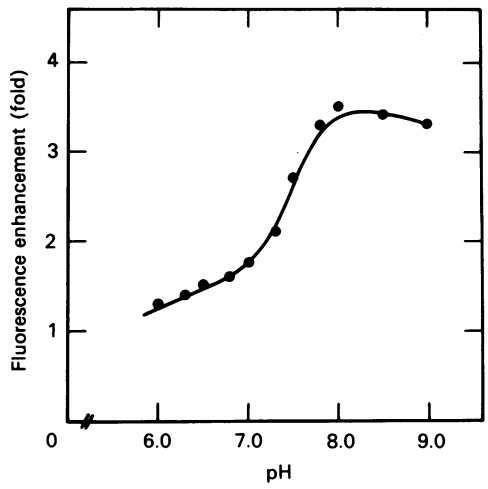

Fig. 6. Enhancement of Tb^{3+} fluorescence induced by β_1-BuTx at pH 6.0–9.0

Fluorescence enhancement is represented by a ratio of Tb^{3+} (0.1 mM) fluorescence in the presence of β_1-BuTx (2.5 μM) to the fluorescence in the absence of β_1-BuTx.

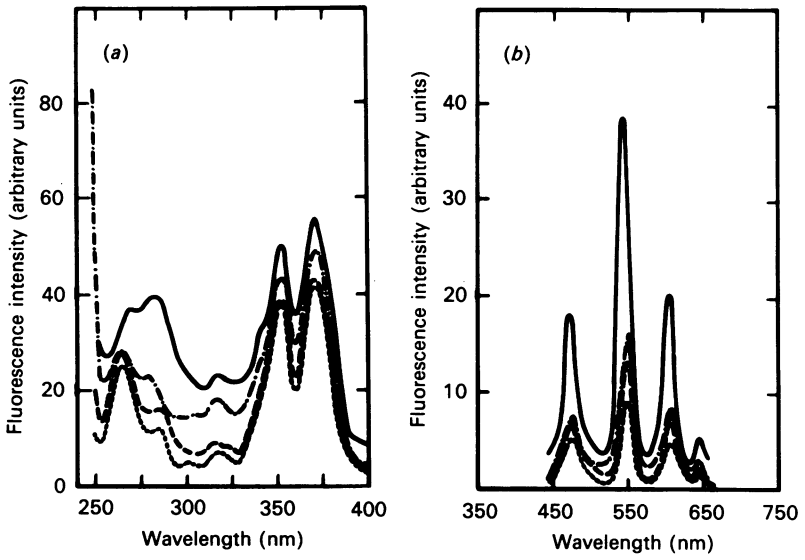

Fig. 5. Fluorescence spectra of Tb^{3+} and the β_1-BuTx–Tb^{3+} complex in 0.02 M-Pipes

(*a*) The excitation spectra were scanned with the emission wavelength at 545 nm. (*b*) The emission spectra were scanned with the excitation wavelength at 295 nm. Tb^{3+} was at 1.0 mM and β_1-BuTx was at 2.5 μM. ·····, Tb^{3+} alone at pH 7.0; ----, Tb^{3+} and β_1-BuTx at pH 7.0; –·–·–, Tb^{3+} alone at pH 7.6; ——, Tb^{3+} and β_1-BuTx at pH 7.6.

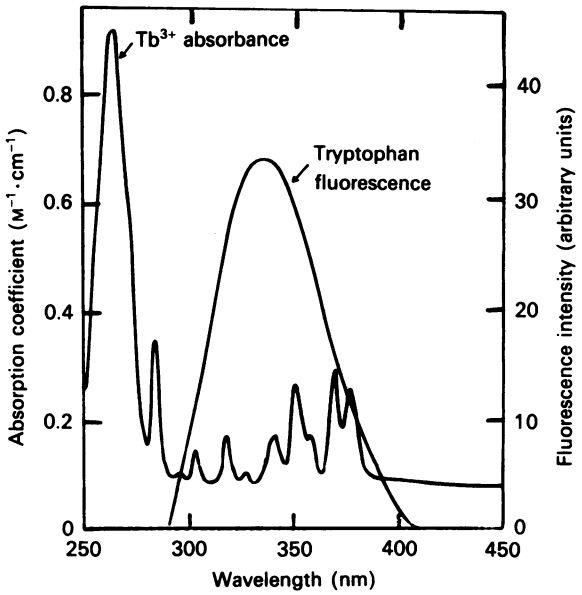

Fig. 7. Spectral overlap between Tb^{3+} absorption and β_1-BuTx Trp-19 fluorescence

The Tb^{3+} absorption spectrum was plotted in terms of molar absorption coefficient. The fluorescence spectrum of β_1-BuTx was plotted in arbitrary units. β_1-BuTx was at 5.0 μM in 0.02 M-Pipes buffer, pH 7.6; $TbCl_3$ was at 1.0 M in the same buffer.

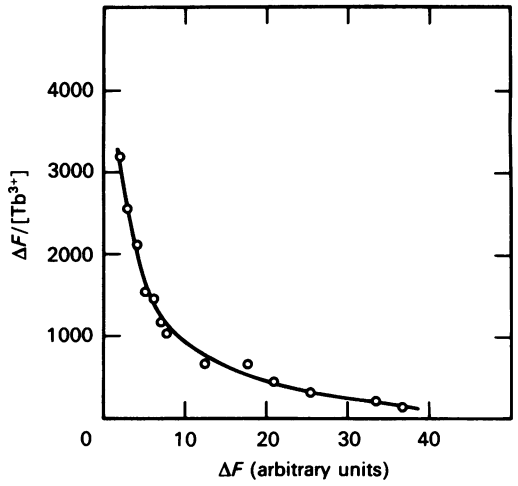

Fig. 8. Modified Scatchard plot for the binding of Tb^{3+} to β_1-BuTx

At pH 7.6 and room temperature, 5.0 μM-β_1-BuTx was titrated with the same solution in the presence of 0.1 M-$TbCl_3$. The fluorescence data were fitted in accordance with eqn. (6) as described in the text.

at 545 nm in the presence of toxin to the fluorescence in the absence of toxin. The enhancement increased slightly from pH 6.0 to 7.0, then followed a remarkable increase in pH 7.0 to 8.0 and levelled off above pH 8.0 (Fig. 6). The middle point of the change was at pH 7.5.

Transfer of resonance energy occurred between Trp-19 and Tb^{3+}. Fig. 7 shows the fluorescence emission spectrum of β_1-BuTx Trp-19 and the absorption spectrum of Tb^{3+}, both at pH 7.6. Since the Tb^{3+} absorption spectrum gave a baseline of $\epsilon = 0.1\ M^{-1}\cdot cm^{-1}$, exclusion of which was taken into account in calculating the overlap integral, J of eqn. (5), in the wavelength region in which the two spectra overlapped. J was calculated to be $0.78 \times 10^{-19}\ M^{-1}\cdot cm^3$. The actual distance between this energy-transfer pair was calculated from eqns. (2) and (4). Q_0 was measured to be 0.186. The refractive index of a globular protein was assumed to be 1.4 (Wallace *et al.*, 1982) and the K^2 value to be 0.331–1.316 for most fluorescent chromophores whose absorption is attributed to triplet degeneracy (Wallace *et al.*, 1982). Thus R_0 of eqn. (4) was calculated to be 0.321–0.404 nm. E of eqn. (3) was determined to be 28 % when λ_1 was 295 nm and λ_2 was 545 nm. Calculation based on eqn. (2) gave R to be 0.376–0.473 nm. At pH 6.3 R was calculated to be 0.486–0.609 nm.

At pH 7.6, 5.0 μM-β_1-BuTx was titrated with the same toxin concentration in the presence of $TbCl_3$. A non-linear curve was obtained in the modified Scatchard plot (Fig. 8), suggesting multiple binding sites of Tb^{3+} on the β_1-BuTx molecule. Taking into account the previous demonstration that the pancreatic PLA_2 molecule has two distinct Ca^{2+}-binding sites (Slotboom *et al.*, 1978; Verheij *et al.*, 1980), we assumed that there were two Tb^{3+}-binding sites on the β_1-BuTx molecule. The association constant of the high-affinity site was calculated to be $2.95 \times 10^3\ M^{-1}$ and that of the low-affinity site was $1.1 \times 10^2\ M^{-1}$. Binding of Tb^{3+} to the low-affinity site was prominent only at high molar ratio of Tb^{3+} to β_1-BuTx, under which condition the enhancement of Tb^{3+} fluorescence was so small that it was not easy to determine the association constant precisely. Our main concern in the following is the high-affinity site.

At pH 7.6 the solution of 5.0 μM-β_1-BuTx and 50.0 μM-Tb^{3+} was titrated with the same solution in the presence of 0.1 M-$CaCl_2$ or 0.1 M-$SrCl_2$, thus keeping the concentration of protein and Tb^{3+} constant. Either bivalent cation could diminish the fluorescence of the β_1-BuTx–Tb^{3+} complex down to that of free Tb^{3+}. The fluorescence data were fitted to eqn. (7). The normalized Scatchard plot for the titration with respect to either Ca^{2+} or Sr^{2+} was considered to be linear (Fig. 9). It was apparent that both ions could compete with Tb^{3+} for the high-affinity site. The association constant of the β_1-BuTx–Ca^{2+} complex was calculated to be $4.25 \times 10^3\ M^{-1}$ and that of the β_1-BuTx–Sr^{2+} complex to be $1.04 \times 10^3\ M^{-1}$. These two values and the association constants of the β_1-BuTx–Tb^{3+} complex had the same order of magnitude, indicating that the three cations could bind to β_1-BuTx with similar affinity. Binding of the cations to β_1-BuTx at pH values lower than 6.8 was found to be weaker than at pH 7.6. At pH 6.8 the association constants were determined to be $3.05 \times 10^2\ M^{-1}$ for the β_1-BuTx–Ca^{2+} complex, $2.45 \times 10^2\ M^{-1}$ for the β_1-BuTx–Tb^{3+} complex and $1.50 \times 10^2\ M^{-1}$ for the β_1-BuTx–Sr^{2+} complex.

PLA_2 activity of β_1-BuTx in the presence of Tb^{3+}

β_1-BuTx showed weak PLA_2 activity. Its activity in 10.0 mM-$CaCl_2$ at 37 °C was 115 units/mg of toxin. This value was comparable with the data of a previous report (Strong *et al.*, 1976). Displacement of Ca^{2+} by Tb^{3+} gave full retention of activity. On the other hand, the activity disappeared almost completely when Sr^{2+} was substituted for Ca^{2+}.

PLA_2 activity of β_1-BuTx was reflected also by its

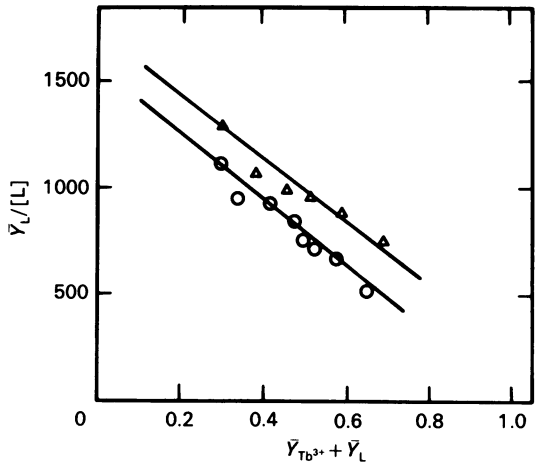

Fig. 9. Normalized Scatchard plot for the binding of Ca^{2+} or Sr^{2+} to β_1-BuTx

A solution of 5.0 μM-β_1-BuTx and 50.0 μM-$TbCl_3$ at pH 7.6 was titrated with the same solution containing 0.1 M-$CaCl_2$ or 0.1 M-$SrCl_2$. The data were treated in accordance with eqn. (7) by linear-regression fitting. The correlation coefficients were calculated to be 0.98 and 0.94 for the β_1-BuTx–Ca^{2+} complex and the β_1-BuTx–Sr^{2+} complex respectively. Symbols: ○, titration with $CaCl_2$; △, titration with $SrCl_2$.

synergistic effect on the haemolysis induced by snake-venom cardiotoxin. We compared the haemolysis of 0.25% human erythrocytes at 40 min incubation at 37 °C by 7.2 μM cobra-venom cardiotoxin with/without 4.0 μM-β_1-BuTx. Cardiotoxin or β_1-BuTx alone in the presence of 0.5 mM-Ca^{2+} or 10.0 μM-Tb^{3+} lysed 5–10% or 10–15% of cells respectively. In the absence of Ca^{2+} or Tb^{3+} or in the presence of 1.0 mM-Sr^{2+} the haemolysis by the two toxins together increased slightly. Under similar conditions addition of Ca^{2+} or Tb^{3+} greatly enhanced the haemolysis: more than 90% of the cells were lysed. This indicated that Tb^{3+} could replace Ca^{2+} to activate the PLA_2 activity of β_1-BuTx but Sr^{2+} could not.

DISCUSSION

According to the empirical rule of Kronman & Holmes (1971), the characteristics of $\lambda_{max.}$ of β_1-BuTx fluorescence and the results of the quenching study on the fluorescence suggest that (a) hydrophobic amino acid residue(s) may cluster around Trp-19, which is proximal to (a) basic amino acid residue(s) but is distant from (an) acidic amino acid residue(s). However, the local conformation around Trp-19 may not be so rigid that it is perturbed upon the binding of metal ions such as Ca^{2+}, Sr^{2+} and Tb^{3+} to the toxin.

β_1-BuTx absolutely requires Ca^{2+} as a cofactor for PLA_2 activity, which is believed to play an essential role in the neurotoxicity (Kelly *et al.*, 1976). The present studies demonstrated that: (1) Ca^{2+} and Tb^{3+} have the same binding site on β_1-BuTx; (2) Tb^{3+} can substitute effectively for Ca^{2+} in the activation of β_1-BuTx PLA_2. These two aspects are important in showing that the fluorescence studies on the binding of Tb^{3+} to the toxin are relevant to Ca^{2+} binding.

The two Tb^{3+}-binding sites on the β_1-BuTx molecule as inferred by us were also independently suggested from the effect of Ca^{2+} on the absorption spectra of β_1-BuTx (Yang & Lee, 1986). The high-affinity and the low-affinity sites may refer to the catalytic site and the interface recognition site of PLA_2 demonstrated in previous studies on the pancreatic PLA_2 (Slotboom *et al.*, 1978; Verheij *et al.*, 1980). Comparing the amino acid residues as part of the catalytic network, which is believed to be preserved in all vertebrate PLA_2 enzymes studied thus far (Kini & Evans, 1987), we suspect that the status of His-48 in the PLA_2 subunit of β_1-BuTx (Fig. 1) may affect the formation of the β_1-BuTx–Tb^{3+} complex (Fig. 6). Since both Ca^{2+} and Tb^{3+} prefer to co-ordinate with oxygen rather than nitrogen atoms (Prados *et al.*, 1974), the imidazole nitrogen atom of His-48 seems not to be a preferred ligand for the ions. In fact, protonation of His-48 does not inhibit formation of the complex completely (Fig. 6). This is supported also by the X-ray studies showing that His-48 of bovine pancreas PLA_2 does not bind to Ca^{2+}, even though it is close to the metal-ion-binding domain (Maraganore *et al.*, 1987). In the β_1-BuTx molecule the Ca^{2+}-binding domain may have a structure such that modification of His-48 with *p*-bromophenylacyl bromide results in the disappearance of the high-affinity site (Yang & Lee, 1986).

Sr^{2+} binds as strongly as Ca^{2+} or Tb^{3+} to β_1-BuTx, but it cannot replace Ca^{2+} in the activation of PLA_2. This might be ascribed to the less marked effect of Sr^{2+} as compared with Ca^{2+} or Tb^{3+} in enhancing polarization of the ester carboxy oxygen atom of the acyl chain of phospholipids in the bond-making process, as proposed in the catalytic mechanism of PLA_2 (Verheij *et al.*, 1980).

It should be stressed that calculation in accordance with eqn. (2) to obtain the distance between the chromophores of an energy-transfer pair is only an estimate. There are uncertainties in the values of factors involved in the calculation. Nevertheless, the estimated distance over which energy transfer occurs for the pair of Trp-19 and Tb^{3+} in the β_1-BuTx molecule reveals two points. First, the indole group of Trp-19 is not close enough to be able to co-ordinate with Ca^{2+}, which binds to Asp-49 as suggested from the previous results of bovine pancreatic PLA_2 (Maraganore *et al.*, 1987). Secondly, protonation of His-48 perturbs the conformation of the active site: it should be noted that the distance between the energy-transfer pair at pH 7.6 is shorter than that at pH 6.3. This may make the metal ion fit less well at the binding site at the lower pH values.

PLA_2 enzymes from the venoms of snakes, scorpions and bees and from mammalian tissues show a high degree of sequence similarity and similar secondary structure (Dufton *et al.*, 1983; Kini & Evans, 1987). A comparison of the tertiary structures of bovine pancreatic PLA_2, pig pancreatic PLA_2 and *Crotalus atrox* PLA_2 shows that the main-chain conformations of the three PLA_2 enzymes are very similar (Dijkstra *et al.*, 1978, 1983; Keith *et al.*, 1981). In the absence of an X-ray structure of β_1-BuTx, we assume that the PLA_2 subunit of β_1-BuTx possesses similar, although not identical, main-chain conformation. We superimpose the primary structure of PLA_2 subunit of β_1-BuTx on to the main chain conformation of PLA_2 enzymes from bovine pancreas and *Crotalus atrox* venom and make some educated guesses (Fig. 1*b*). The molecule has the shape of a rectangular box with dimensions of approx. 2.5 nm × 2.8 nm × 3.5 nm (Dijkstra *et al.*, 1978). It is possible for the indole group of Trp-19 to lie relatively near to either the carboxylic group of Asp-49 or the

imidazole group of His-48. This configuration seems to be compatible with the nature of the energy-transfer pair of Tb^{3+} and Trp-19.

This work was partially supported by the National Science Council, Taiwan, Republic of China (Grant NSC 77-0412-B-001-02). Some of the work described in this paper forms part of a dissertation submitted by S.-T. C. in partial fulfilment for the requirement of the degree of D.Sc. at the National Taiwan University.

REFERENCES

Abe, T., Alema, S. & Miledi, R. (1977) Eur. J. Biochem. **80**, 1–12

Chang, C. C. (1985) Proc. Natl. Sci. Counc. Repub. China Part B **9**, 126–142

Chen, Y. H., Tai. J. C., Huang, W. J., Lai, M. Z., Hung, M. C., Lai, M. D. & Yang, J. T. (1982) Biochemistry **21**, 2592–2600

Chen, Y. H., Liou, R. F., Hu, C. T., Juan, C. C. & Yang, J. T. (1987) Mol. Cell. Biochem. **73**, 69–76

Dijkstra, B. W., Drenth, J., Kalk, K. H. & Vandermaelen, P. J. (1978) J. Mol. Biol. **124**, 53–60

Dijkstra, B. W., Renetseder, R., Kalk, K. H., Hol, W. G. J. & Drenth, J. (1983) J. Mol. Biol. **168**, 163–179

Dufton, M. J. (1985) Eur. J. Biochem. **153**, 647–654

Dufton, M. J., Eaker, D. & Hider, R. C. (1983) Eur. J. Biochem. **137**, 537–544

Epstein, M., Levitzki, A. & Reuben, J. (1974) Biochemistry **13**, 1777–1782

Forster, T. (1959) Discuss. Faraday Soc. **27**, 7–17

Freifelder, D. (1982) in Physical Biochemistry (Freifelder, D., ed.), p. 554, W. H. Freeman, San Francisco

Gergely, J., Horrocks, W., DeW., Leavis, P. C. & Wang, C. L. (1981) Biochemistry **20**, 2439–2444

Harvey, A. L. & Karlsson, E. (1982) Br. J. Pharmacol. **77**, 153–161

Received 4 January 1989/11 April 1989; accepted 26 April 1989

Ikeda, K. & Hayashi, K. (1983) J. Biochem. (Tokyo) **93**, 1343–1351

Keith, C., Feldman, D. S., Deganello, S., Glick, J., Ward, K. B., Johnes, E. O. & Sigler, P. B. (1981) J. Biol. Chem. **256**, 8602–8607

Kelly, R. B., Oberg, S. G., Strong, P. N. & Wagner, G. M. (1976) Cold Spring Harbor Symp. Quant. Biol. **40**, 117–125

Kini, R. M. & Evans, H. J. (1987) J. Biol. Chem. **262**, 14402–14407

Kondo, K., Narita, K. & Lee, C. Y. (1978*a*) J. Biochem. (Tokyo) **83**, 91–99

Kondo, K., Narita, K. & Lee, C. Y. (1978*b*) J. Biochem. (Tokyo) **83**, 101–115

Kondo, K., Toda, H., Narita, K. & Lee, C. Y. (1982) J. Biochem. (Tokyo) **91**, 1531–1548

Kronman, M. J. & Holmes, L. G. (1971) Photochem. Photobiol. **14**, 113–134

Lehrer, S. S. (1971) Biochemistry **10**, 3254–3262

Lin, W. Z., Chu, S. T. & Chen, Y. H. (1984) Proc. Natl. Acad. Sci. Counc. Repub. China Part B **8**, 113–118

Maraganore, J. M., Poorman, R. A. & Heinrikson, R. L. (1987) J. Protein Chem. **6**, 173–189

Prados, R., Stadtherr, L. G., Donatos, H., Jr. & Martin, R. B. (1974) J. Inorg. Nucl. Chem. **36**, 689–693

Slotboom, A. J., Jansen, E. H. J. M., Vlijm, H., Pattus, F., Soares de Araujo, P. & de Haas, G. H. (1978) Biochemistry **17**, 4593–4600

Strong, P. N., Goerke, J., Oberg, S. G. & Kelly, R. B. (1976) Proc. Natl. Acad. Sci. U.S.A. **73**, 178–182

Verheij, H. M., Volwerk, J. J., Jansen, E. H. J. M., Puyk, W. C., Dijkstra, B. W., Drenth, J. & de Haas, G. H. (1980) Biochemistry **19**, 743–750

Verheij, H. M., Slotboom, A. J. & de Haas, G. H. (1981) Rev. Physiol. Biochem. Pharmacol. **91**, 91–203

Wallace, R. W., Tallant, E. A., Dockter, M. E. & Cheung, W. Y. (1982) J. Biol. Chem. **257**, 1845–1854

Yang, C. C. & Lee, H. J. (1986) J. Protein Chem. **5**, 15–28